VIBRATION REDUCTION IN HELICOPTER ROTOR WITH DYNAMIC STRESS CONSTRAINTS USING RESPONSE SURFACE METHODS

M. Senthil Murugan* and Ranjan Ganguli+

Abstract

An optimization procedure to reduce oscillatory hub loads for a four bladed soft-inplane hingeless helicopter rotor is developed. The objective function to be minimized consists of scalar norms of 4/rev vibratory hub loads transmitted by a 4-bladed helicopter rotor to the fuselage. The mass and stiffness properties of the rotor blades are considered as the design variables. Constraints are imposed on the dynamic stresses caused by the blade root loads, and move limits on the design variables. An aeroelastic analysis based on finite elements in space and time is used to construct the response surface approximation for the objective function and constraints. The response surface approximations decouple the analysis problem from the optimization problem. The numerical sampling is done using the central composite design of the theory of design of experiments. The approximate optimization problem expressed in terms of response surfaces is solved using genetic algorithms. Optimization results in forward flight with unsteady aerodynamic modeling show a reduction in the objective function of about 15 percent. The dominant loads in vehicle vibration are the vertical hub shear and the rolling and pitching moments which are reduced by 22-26 percent. This paper proposes a multidisciplinary design which is suited to industrial application due to the decoupling of the analysis and optimization problems.

Keywords : Helicopter, Response surface approximations, Aeroelastic analysis, Vibration reduction, Genetic algorithms

Introduction

In a helicopter, the main rotor is the crucial subsystem, which provides lift, propulsive force and control capability of the helicopter. Therefore, the design of main rotor is an important problem that has received considerable attention. The design of the helicopter rotor involves a variety of aerospace engineering disciplines. Rotor blades are slender flexible beams, which can undergo elastic deformations in bending and torsion, that can be beyond the limits of linear beam theories. The deflections of the blade interact with the aerodynamic loading. The rotor blade aerodynamics in turn, is coupled with the structural dynamics because much of the elastic deformation and damping in flap and lag bending and in torsion is of aerodynamic origin. Therefore, the prediction of helicopter blade and hub loads is an integrated aeroelastic problem. Helicopter rotor aeroelastic analysis have been developed by academic institutions and helicopter companies are widely used for preliminary design of the helicopter rotor blades.

One of the chief issues in the helicopter industry is the minimization of vibrations on the helicopter airframe, which are caused by an unsteady aerodynamic environment and highly flexible rotating blades. The vibratory bending moments acting along the blade length also causes dynamic stresses, at several harmonics of the rotational speed, on the rotor blade. These dynamic stresses cause structural fatigue, leading to a reduction in blade life. The critical dynamic stresses generally occur at the spanwise location where the vibratory bending moment is highest. For the hingeless rotors, it occurs at the blade root. Therefore, a direct approach for increasing the life of the blade is to design the rotor to produce low vibratory bending moments. The changes of mass and stiffness along the blade chord and span direction affect the structural dynamics and aeroelastic behaviour as well as the stress distribution.

* M.Sc. (Engg) Student +Assistant Professor
Department of Aerospace Engineering, Indian Institute of Science, Bangalore-560 012, India
Manuscript received on 14 Jul 2003; Paper reviewed, revised and accepted on 22 Mar 2004

In recent years, considerable research has been directed towards the application of aeroelastic optimization methodology for the vibration reduction problem. Ganguli and Chopra [1,2] carried out aeroelastic optimization studies out for rotor blades with swept tips and for composite rotors. Yaun and Friedmann [3,4] carried out a structural optimization study for vibration reduction of a composite rotor blade with a swept tip. Chattopadhyay et.al [5]-[11] have done extensive work on the optimization of helicopter rotors and prop rotors. Non-gradient methods in engineering optimization have become popular among the researchers in recent years because of their ability in finding the global minima and permitting the use of integer and discrete design variables. The most popular non-gradient methods are genetic algorithm and simulated annealing [12]. Lee and Hajela [13] applied genetic algorithm for the rotor design problems. Other recent studies in helicopter rotor optimization includes those by Kim and Sarigul-Klijn [14] - [17] for articulated rotors, Soykasap and Hodges [18] for composite tilt rotors, and Celi et.al [19] - [21] addressing maneuver flight. A recent review on helicopter optimization is provided by Celi [22].

The helicopter rotor dynamics analysis involves complex computer analyses, which are computationally expensive to perform. These analyses involve the solution of nonlinear rotor dynamics equation, obtaining the helicopter trim condition and aeroelastic stability condition. In the conventional aeroelastic optimization studies, the large aeroelastic analysis program has to be integrated with the optimization software, which can make the problem a cumbersome task. Gradient based approaches to optimization require that the sensitivity derivatives either be calculated analytically or by finite difference. Finite difference derivatives are computationally expensive to calculate and the selection of an appropriate step size can be difficult. Analytical and semi analytical derivatives have been used by Spence and Celi [21], Murthy and Lu [23], Lim and Chopra [24], and Ganguli and Chopra [1,2,29]. These derivatives are obtained using chain rule differentiation and included in the computer program for aeroelastic analysis as an integral part. Analytical derivatives are more accurate than finite differences and large savings of computer time are possible. However certain approximations such as ignoring the changes in trim conditions and blade normal modes due to changes in design variables are often made in calculation of analytical derivatives. These assumptions appear to have been reasonable for the vibration reduction problems. A key problem of analytical derivatives is linked to the issue of the software aging. With the passage of time, changes are made in the aeroelastic analysis to account for refinements in physical modeling. When such changes are made, the analytical derivatives must also be updated. This is not always possible as the domain experts performing physical modeling may not be aware of the optimization aspects of the software. Furthermore, in the industry setting the rotor aeroelastic analysis codes are considered as proprietary and it is very difficult to make changes inside them. Therefore analytical derivatives are difficult to implement in an industry setting.

One approach to overcome this difficulty is to use statistical techniques to construct approximations of the analyses that are much more efficient to run and easier to integrate together, and yield insight into the functional relationship between the objective function and design variables [25]. This results in the construction of the approximations of the analyses, instead of integrating the computer programs. Response Surface (RS) methodology is one such statistical method used to construct approximations [26]. Response surfaces for objective and constraint functions are created by sampled numerical experiments over the design space [27]. The response surface models created then replaces the computationally expensive analyses and facilitates fast analysis and exploration of the design space. Low order polynomials are mostly used as the response surface approximating functions. In helicopter aeroelastic optimization very limited work has been done using response surfaces. Henderson, Walsh and Young [28] have applied response surface techniques to helicopter rotor blade optimization. Hajela et.al [13] also used neural surrogate functions in rotor blade optimization.

The objective of this study is to perform an aeroelastic optimization of a helicopter rotor, using response surface approximations. The helicopter aeroelastic analysis is based on a finite element method in space and time. To reduce helicopter vibrations, the objective function includes all six components of 4P hub loads for a four bladed hingeless rotors, while maintaining the constraints on dynamic stresses developed on the rotor blade, which are caused primarily by the 1/rev and 2/rev rotating frame loads. This paper approaches the problem of vibration reduction by developing an RS model for the objective function, instead of doing the rotor dynamic analysis for each function evaluation required by the optimization process. Considering the design space for rotor design problems are often non-convex and that design variables for actual rotor cross sections could be continuous, discrete or integer in nature, Genetic Algorithms (GA) are

used, for the optimization process [30], GA requires many function evaluations and can be computationally very expensive if directly applied to the helicopter problem. However, the RS polynomial approximations used in this study makes the cost of function evaluation very less.

Helicopter Rotor Dynamic Analysis

In this work, a comprehensive aeroelastic analysis code, based on finite element method is used to evaluate the resultant forces of the rotor. The rotorcraft structure is modeled as a nonlinear representation of elastic rotor blades coupled to a rigid fuselage. The blade is modeled as a slender elastic beam undergoing flap bending, lag bending, elastic twist, and axial deflection. The effect of moderate deflections is included by retaining second order nonlinear terms[31]. Governing equations are derived using a generalized Hamilton's principle applicable to non-conservative systems [31].

$$\int_{\psi_1}^{\psi_2} (\delta U - \delta T - \delta W)\, d\psi = 0 \qquad (1)$$

The δU , δT and δW are virtual strain energy, kinetic energy, and virtual work, respectively. The δU and δT include energy contribution from components that are attached to the blade. External aerodynamic forces on the blade contribute to the virtual work variational, δW. The aerodynamic forces and moments are calculated using quasi-steady/unsteady aerodynamics. Finite element method is used to discretize the governing equations of motion, and allows for accurate representation of complex hub kinematics and non-uniform blade properties [32]. After the finite element discretization, Hamilton's principle is written as

$$\int_{\psi_i}^{\psi_f} \sum_{i=1}^{N} (\delta U_i - \delta T_i - \delta W_i)\, d\psi = 0 \qquad (2)$$

Each of the N beam elements has fifteen degrees of freedom. These degrees of freedom are distributed over five element nodes (2 boundary nodes and 3 interior nodes). There are six degrees of freedom at each element boundary node. There are two internal nodes for axial deflection and one internal node for elastic twist. Between elements there is continuity of displacements and slope for flap and lag bending deflections, and continuity of displacement for elastic twist and axial deflections. These elements ensure physically consistent linear variations of bending moments and torsional moment, and quadratic variation of axial force within each element. Using the interpolating polynomials, the distribution of deflections over a beam element is expressed in terms of the elemental nodal displacements. The shape functions used are Hermite polynomials for lag and flap bending, and Lagrange polynomials for axial and torsion deflection [37].

Assembling the blade finite element equations and applying boundary conditions results in equation (2) becoming [32],

$$M\, \ddot{q}(\psi) + C\, \dot{q}(\psi) + K q(\psi) = F(q, \dot{q}, \psi) \qquad (3)$$

The nodal displacement **q** are functions of time and all non-linear terms have been moved into the force vector on the right hand side. The spatial functionality has been removed by using finite element discretization and partial differential equations have been converted into ordinary differential equations.

The finite element equations representing each rotor blade are transformed to normal mode space for efficient solution of blade response using the modal expansion. Typically, 6-10 modes are used. The displacements are expressed in terms of normal modes as

$$q = \Phi p \qquad (4)$$

Substituting equation (4) into equation (3) lead to normal mode equations having the form

$$\overline{M}\, \ddot{p}(\psi) + \overline{C}\, \dot{p}(\psi) + \overline{K}\, p\, (\psi) = \overline{F}(p, \dot{p}, \psi) \qquad (5)$$

These equations are non-linear ODE's but their dimensions are much reduced compared to the full finite element equations (3). The normal mode mass, stiffness and damping matrix and force vectors are given by

$$\overline{M} = \Phi^T M \Phi\,,\ \overline{C} = \Phi^T C \Phi\,,\ \overline{K} = \Phi^T K \Phi\,,\ \overline{F} = \Phi^T F \qquad (6)$$

The mode shapes or eigen vectors on equation (4) and (6) are obtained from rotating frequencies of the blade [32].

$$K_s \Phi = \omega^2 M_s \Phi \qquad (7)$$

The blade normal mode equation (5) can be written in the following variational form [24]

$$\int_0^{2\pi} \delta p^T \left(\bar{M}\ddot{p} + \bar{C}\dot{p} + \bar{K}p - \bar{F} \right) d\psi = 0 \qquad (8)$$

Integrating equation (8) by parts, we obtain [24]

$$\int_0^{2\pi} \begin{Bmatrix} \delta p \\ \delta \dot{p} \end{Bmatrix} \begin{Bmatrix} \bar{F} - \bar{C}\dot{p} - \bar{K}p \\ \bar{M}\dot{p} \end{Bmatrix} d\psi = \begin{Bmatrix} \delta p \\ \delta \dot{p} \end{Bmatrix} \begin{Bmatrix} M\dot{p} \\ 0 \end{Bmatrix}_0^{2\pi} \qquad (9)$$

Since the helicopter rotor is a periodic system with a time period of one revolution, we have $\dot{p}(0) = \dot{p}(2\pi)$. Imposing periodic boundary conditions on equation (9) results in the right hand side becoming zero and yields the following system of first order ordinary differential equations [24] :

$$\int_0^{2\pi} \delta y^T Q \, d\psi = 0 \qquad (10)$$

where

$$y = \begin{Bmatrix} p \\ \dot{p} \end{Bmatrix}, \quad Q = \begin{Bmatrix} \bar{F} - \bar{C}\dot{p} - \bar{K}p \\ \bar{M}\dot{p} \end{Bmatrix} \qquad (11)$$

The non-linear, periodic, ordinary differential equations are then solved for blade steady response using the finite element in time method [36] and a Newton-Raphson procedure [24]. Discretizing equation (11) over N_t time elements around the rotor disk (where $\psi_1 = 0$, $\psi_{N_{t+1}} = 2\pi$) and taking first order Taylor series expansion about the steady state value $y_o = \left[p_o^T \; \dot{p}_o^T \right]$ yields algebraic equations [24]

$$\sum_{i=1}^{N_t} \int_{\psi_i}^{\psi_{i+1}} \delta y_i^T Q_i (y_0 + \Delta y) \, d\psi$$

$$= \sum_{i=1}^{N_t} \int_{\psi_i}^{\psi_{i+1}} \delta y_i^T \left[Q_i (y_0) + K_{ti} (y_0) \Delta y \right] d\psi = 0, \qquad (12)$$

where

$$K_{ti} = \begin{bmatrix} \dfrac{\partial \bar{F}}{\partial P} - \bar{K} & \dfrac{\partial \bar{F}}{\partial \dot{P}} - \bar{C} \\ 0 & \bar{M} \end{bmatrix}_i \qquad (13)$$

For the ith time element, the modal displacement vector can be written as

$$p_i(\psi) = H(s)\xi_i, \qquad (14)$$

where H(s) are time shape functions [36] which are fifth order lagrange polynomials [24] used for approximating the normal mode coordinate p. For a fifth order polynomial, six nodes are needed to describe the variation of p within the element. Continuity of generalized displacements is assumed between the time elements. Substituting equations (14) and its derivative into equation (13) yields the time discretized blade response [24]

$$Q^G + K_i^G \Delta \xi^G = 0, \qquad (15)$$

where

$$Q^G = \sum_{i=1}^{N_t} \int_{\psi_i}^{\psi_{i+1}} H^T Q_i \, d\psi, \qquad (16)$$

$$K_t^G = \sum_{i=1}^{N_t} \int_{\psi_i}^{\psi_{i+1}} H^T \begin{bmatrix} \dfrac{\partial \bar{F}}{\partial P} - \bar{K} & \dfrac{\partial \bar{F}}{\partial \dot{P}} - \bar{C} \\ 0 & \bar{M} \end{bmatrix}_i d\psi,$$

$$\Delta \xi^G = \sum_{i=1}^{N_t} \Delta \xi_i$$

Solving the above equations iteratively yields the blade steady response.

Steady and vibratory components of the rotating frame blade loads (i.e., shear forces and bending/torsion moments) are calculated using the force summation method [33]. In this approach, blade inertia and aerodynamic forces are integrated directly over the length of the blade. Fixed frame hub loads are calculated by summing the individual contributions of individual blades [34].

Once the hub loads are obtained the helicopter needs to be trimmed. This is defined as the condition where the steady forces and moments acting on the helicopter sum to zero and simulates the condition for steady level flight [35]. The trim solution for the helicopter involves finding the pilot controls angles θ at which the six steady forces and moments acting on the helicopter are zeros :

$$F(\theta) = 0 \tag{17}$$

These nonlinear trim equations are also solved using the Newton-Raphson method. The helicopter rotor trim equations and the blade response equations and are solved simultaneously to obtain the blade steady response and hub loads. This coupled trim procedure is important for capturing the aeroelastic interaction between the aerodynamic forces and the blade deformations. Further details of the analysis are available from the UMARC reference [37].

Response Surface Modeling

Response surface modeling techniques have been used in the past few years to solve complex, computationally intensive engineering problems [38]. Design of Experiments (DOE) theory provides a systematic means of selecting the set of points in the k dimensional design space, at which to perform computational analyses. By using the RS techniques, the analysis codes are separated from the optimization codes. The complex analysis codes are replaced by the simple polynomials. Second order or quadratic polynomials are mostly used. The Hessian of these second order polynomials may be positive definite or negative definite or indefinite. A quadratic RS model in k variables of the form,

$$y = \beta_0 + \sum_{i=1}^{k} \beta_i x_i + \sum_{i=1}^{k} \sum_{j=1}^{i} \beta_{ij} x_i x_j \tag{18}$$

is used in this paper. The second order model described in the above equation is a widely used model to describe experimental data in which system curvature is readily abundant. The above model of equation contains $1 + 2k + k(k\text{-}1)/2$ parameters. As a result, the experimental design used must contain at least $1+2k+k(k\text{-}1)/2$ distinct design points. In addition, the design must involve at least three levels of each design variable to estimate the pure quadratic terms. There are families of designs available, for fitting the second order model. The central composite designs (CCDs) is one of the popular class of second-order designs. It involves the use of a two level factorial or fraction combined with the $2k$ axial or star points. As a result, the design involves, 2^k factorial points, $2k$ axial points, and n_c center runs. The factorial points represent a variance optimal design for a first order model or a first-order+two-factor interaction type model. Center runs provide information about the existence of curvature in the system. If curvature is found in the system, the addition of axial points allow for efficient estimation of the pure quadratic terms. The choice of α, the axial distance, depends to a great extent on the region of operability and region of interest. The values of axial distance varies from 1.0 to $\sqrt{k}$. For the $k = 2$ case the value of α, the axial distance is $\sqrt{2}$. Fig.1 shows the CCD for $k = 2$. In this case, for $k = 2$, there are $4(2^k)$ factorial points, 4 $(2*k)$ axial points and one center point resulting in 9 points. Also note that for $k = 2$, there are $1+2k+k(k\text{-}1)/2 = 6$ regression coefficients need to be determined to find the second order response surface as showing in equation (27). The CCD design therefore overfits the points to obtain the response surface. It is therefore able to reduce the error present in any one of the points and avoid the local minima that are not robust and have high sensitivity to change in the design variables.

Once the objective function values have been evaluated at the CCD points, the response surface model has to be fitted with these data. The method of least squares is typically used to estimate the unknown coefficients in the response surface model [38]. The response surface model given in the equation (18) can be written in matrix notation as

$$y = X\beta + \varepsilon \tag{19}$$

where **y** is an (n x 1) vector of observations, **X** is an (n x p) matrix of the levels of the independent variables, β is a

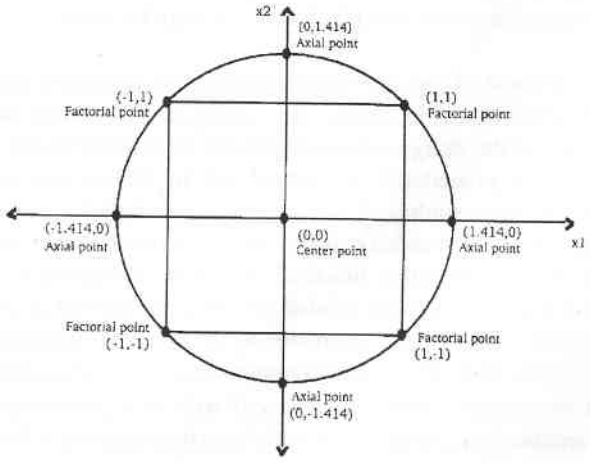

Fig.1 Central composite design for k = 2

(p x 1) vector of the regression coefficients and ε is a (p x 1) vector of error terms. The regression coefficients can be obtained by minimizing the least squares error obtained using the equation (19) as follows :

$$L = \sum_{i=1}^{n} \varepsilon^2 = \varepsilon' \varepsilon = (y - X\beta)' (y - X\beta)$$

$$= y' y - 2\beta' X'y + \beta' X'y \qquad (20)$$

The least squares estimator must satisfy [38]

$$\frac{\partial L}{\partial \beta}\Big|_b = -2 X'y + 2 X' b = 0 \qquad (21)$$

which simplifies to

$$X' Xb = X'y, \quad b = (X'X)^{-1} X'y \qquad (22)$$

The fitted regression model is

$$\hat{y} = X b \qquad (23)$$

The difference between observation and fitted value is the residual and is given as [38]

$$\varepsilon = y - \hat{y} \qquad (24)$$

While there are formal methods of estimating the error in the response surfaces, engineering judgment can often be used to account for the accuracy for the fitted model. The second order response surface model given in equation (18) can easily capture the curvature of the actual response and can identify the region of optimum in the design space even-though the error ε may be more.

In most of the aeroelastic optimization problems, the objective function cannot be expressed analytically in terms of the design variables. Therefore, numerical optimization procedures are carried out in the aeroelastic optimization studies. A large number of aeroelastic simulations may be needed in the numerical optimization process for the objective function evaluation. However, the number of simulations needed for fitting the second order response surface approximation to the objective function using CCD are lesser. For example, in a two variable case, if the design space is considered with ±10 percentage variation for each design variable from their baseline value and the design space is divided with 5% variation, the number grid points generated will be 25. Therefore, if exhaustive search method is employed in optimization, the aeroelastic analysis has to be performed at these 25 grid points for finding the optima within the design space. In the same design space, the CCD requires only 9 points for fitting the second order model approximation to the objective function. Therefore, the aeroelastic simulation has to be performed only at these 9 points compared to the 25 aeroelastic simulations needed in the exhaustive search method. The response surface approximation created with these 9 CCD points is used for objective function evaluation in the optimization process.

Genetic Algorithm

The aeroelastic optimization of helicopters which were intractable a few years ago have become tractable today with the rapidly growing power of computers. In recent years, GA has been used in the helicopter optimization [39] - [45]. In these algorithms, the design variables are expressed as strings of 0's and 1's; these bit can be the exponents of 2 in a binary representation. The strings corresponding to each variable are then joined together to form a long binary string that defines the entire design. The GA starts with a certain number of initial design strings with random combinations of 0's and 1's. The algorithm then proceeds by generating new designs with bit operations devised to mimic mathematically some biological evolutionary phenomena, such as mating, crossover, and mutation. Through these operations the design evolves towards the optimum. GA can deal with integer and discrete variables. Also, they have a better likelihood to identify global minima than conventional gradient-based algorithms. A comprehensive introduction to GA is provided by Goldberg [30] and a recent review on non-gradient methods is given by Hajela [12].

In this work, the constraints were appended to the objective function $f(x)$, using a quadratic exterior penalty function, which is of the form

$$P(X) = f(X) + \sum_{j=1}^{J} u_j \max[0, g_j(X)]^2 + \sum_{k=1}^{K} v_k (h_k(X))^2 \qquad (25)$$

where $g_j(X)$, $h_k(X)$ are the equality and inequality constraints, respectively expressed in the form, $g_j(X) \le 0$ and $h_k(X) = 0$. The u_j and v_k represents the penalty parameters. The exterior penalty method is widely used in practice and well suited for GA. The GA does not have the problems of highly nonlinear variations along the constraint boundaries, which result when the exterior penalty functions are used in the gradient based methods [46].

Problem Description

The objective function J_v used in this study represents the vibratory hub loads and has been used widely in the rotorcraft vibration [1] - [4]. The objective function is the sum of the scalar norms of the N/rev forces and the N/rev moment's transmitted by an N-bladed helicopter rotor to the fuselage as the primary source of vibration. In this work, 4/rev hub force resultant and, 4/rev hub moment resultant of a four bladed rotor is used as the objective function J_v. The objective function is of the form

$$f(X) = J_v = \sqrt{(F_x^{4p})^2 + (F_y^{4p})^2 + (F_z^{4p})^2} + \sqrt{(M_x^{4p})^2 + (M_y^{4p})^2 + (M_z^{4p})^2} \quad (26)$$

where the forces and moments are non-dimensionalized with respect to $m_0 \Omega^2 R^2$ and $m_0 \Omega^2 R^3$, respectively. In the above equation F_x, F_y and F_z represents the longitudinal, lateral and vertical dynamic forces acting on the hub and, M_x, M_y and M_z are the rolling, pitching and yawing moments acting on the hub, respectively.

In the helicopter rotor, the loads observed in the rotating frame are periodic and can be expressed in terms of Fourier series. The first harmonic of these loads in the rotating frame is generally dominant and the magnitude of the harmonics declines with the higher harmonics. The 4/rev hub loads in the fixed frame come from the 3/rev, 4/rev and 5/rev in the rotating frame. Attempts to minimize the 4/rev hub loads for a four bladed hingeless rotor in forward flight can result in an increase in the 1/rev and 2/rev blade loads, causing higher dynamic stresses. The lower harmonic blade loads which are higher in magnitude are the main sources of dynamic stresses. Therefore, the constraints are imposed on the dynamic stresses caused by the 1/rev and 2/rev blade root bending moments. These constraints avoid reducing the fatigue life of the blade. The constraints are given by

$$J_{d1}^{i} \le J_{d1}^{o} \quad (27)$$

$$J_{d2}^{i} \le J_{d2}^{o} \quad (28)$$

where J_{d1}^{i} , J_{d2}^{i} are the scalar norm of 1/rev and 2/rev blade root bending moments at the i^{th} iteration of optimization, which are given below :

$$J_{d1}^{i} = \left[\sqrt{(F_x^{1p})^2 + (F_y^{1p})^2 + (F_z^{1p})^2} + \sqrt{(M_x^{1p})^2 + (M_y^{1p})^2 + (M_z^{1p})^2}\right]^2 \quad (29)$$

$$J_{d2}^{i} = \left[\sqrt{(F_x^{2p})^2 + (F_y^{2p})^2 + (F_z^{2p})^2} + \sqrt{(M_x^{2p})^2 + (M_y^{2p})^2 + (M_z^{2p})^2}\right]^2 \quad (30)$$

Here J_{d1}^{0} , J_{d2}^{0} are the baseline values of the same 1/rev and 2/rev dynamic stresses respectively. To ensure the design variables stay within the region where the response surface is valid, a constraint is added. For the two design variables, it is found that constraining the design variables with in the circle as shown in the Fig.1 is effective. And the constraint is given by,

$$x_1^2 + x_2^2 \le 2 \quad (31)$$

where the x_1 and x_2 are coded variables used in the design of experiments and can be converted to physical variables using a linear transformation. For example, the levels +1 and -1 of the coded variable x_1 in the Fig.1 can correspond to 5 percent increase and decrease from the baseline value of the blade mass, respectively. The baseline value of the mass corresponds to the center point in the x_1 direction. Similarly for the coded variable x_2, the +1 and -1 can correspond to 25 percent increase and decrease from the baseline value of the torsional stiffness. Therefore, once the baseline design at the center point is selected, the factorial points can be defined as percent changes in the baseline and the axial points are calculated using a linear transformation.

Expanding the formulation (31) to k design variables, the constraint can be expressed in the form,

$$x_1^2 + x_2^2 + x_3^2 + \ldots + x_k^2 \le k \quad (32)$$

The design variables are constrained to remain with in the hypersphere of radius $\sqrt{k}$. The three constraints used in this work can be written in standard notation as,

$$g_1(X) = J_{d1}^{i} - J_{d1}^{0}$$
$$g_2(X) = J_{d2}^{i} - J_{d2}^{0}$$
$$g_3(X) = \sum_{i=1}^{k} x_i^2 - k \quad (33)$$

The composite objective function can then be written as,

$$P(X) = f(X) + u_1 [\max (0, g_1 (X))]^2$$

$$+ u_2 [\max (0, g_2 (X))]^2 + + u_3 [\max (0, g_3 (X))]^2 \quad (34)$$

where are u_1, u_2 and u_3 are the penalty parameters and a numerical value of 100 has been taken for each, to obtain the numerical results discussed in the next section.

Results and Discussion

For the numerical study, a four bladed soft-inplane hingeless rotor blade which is uniform blade equivalent of the BO105 rotor blade is considered. The rotor properties used in this study are shown in the Table-1.

An advance ratio of 0.3, which simulates forward flight condition is used to obtain the numerical result.

Two Design Variables

To have the geometric representation of the RS model and a better understanding of the method, only two design variables are considered initially. These variables are selected as the blade mass and the torsional stiffness, and are selected as they have been observed to have a strong influence on rotor vibration from earlier studies [1,2]. The Lock number has to be updated with the change in the values of the mass. The Lock number (γ) is defined as

Table-1 : Baseline Hingeless Blade Properties	
Number of blades	4
Radius (m)	4.94
Hover tip speed, m/s	198.12
m_o (kg/m)	6.46
$EI_y/m_o \Omega^2 R^4$	0.0108
$EI_z/m_o \Omega^2 R^4$	0.0268
$GJ/m_o \Omega^2 R^4$	0.00615
m/m_o	1.0
Lock number	5.2
solidity	0.07
C_T/σ	0.07
c/R	0.055

$\gamma = \rho\, acR^4/I_b$. Here ρ is density of the air, a is the lift curve slope, c is the blade chord, R is the rotor radius and I_b is the mass moment of inertia of the rotor blade. Thus, as the blade mass changes I_b changes resulting in a change in the Lock number.

The optimization is carried out for two cases. In the first case, quasi-steady aerodynamic model is employed in the rotor analysis and in the second case, unsteady aerodynamic model with both attached flow and impulsive aerodynamics is used. The unsteady aerodynamics are based on the Leishman model [47].

Case 1 : Quasi-Steady Aerodynamic Model

In previous studies, quasi-steady aerodynamics has been used in the rotor dynamic analysis [1,2]. To see the influence of the unsteady aerodynamic model, optimization is carried out first with the quasi-steady model. A variation of 25 and 5 percent is taken from the baseline values of torsional stiffness and the mass of the blade, respectively. As per the DOE theory, 9 (i.e, 2^2+2* 2 +1=9) points are selected in the design space. The objective function values are evaluated at the selected in the design space. The objective function values are evaluated at the selected points, using the UMARC code. A RS model is developed with these results, which is shown in the Fig.2, where the GJ and m represents the torsional stiffness and the blade mass, respectively. The second order response surface function is also given at the bottom of the figure.

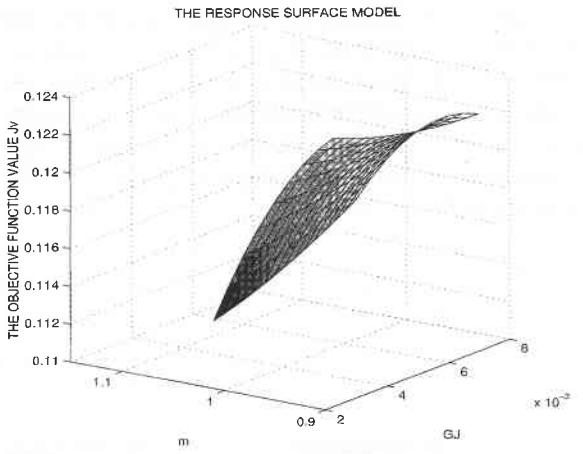

Fig.2 RS with quasisteady model about baseline design ($\Delta GJ = 25\%$,$\Delta m = 5\%$) $J_v = 0.2719 - 3.9027\, GJ - 0.2520\, m - 338.4307\, GJ^2 + 0.08\, m^2 + 9.106\, GJ{*}\, m$

Then optimization is carried out using GA. In GA, the two design variables were represented with a total of 20 bits, each with 10 bits. The other GA parameters used are given in the Table-2. Constraints are imposed on the function to ensure that the design variables remain in the region, where the response surface is valid. This is assured by constraining the design variables to remain in the circle as shown in the Fig.1. The results of the optimization shows a reduction of 4.08% in the objective function value J_v. And the non-dimensional optimum design values are GJ = 0.004454, m = 1.0442. The reduction is achieved with a decrease in the torsional stiffness and a slight increase in the mass from the baseline design value.

Case 2 : Unsteady Aerodynamic Model

In this case, and for all future results, unsteady aerodynamic model is employed in the rotor analysis code. To search for the global minima, the optimization is carried out in different stages. The size of the design space is reduced in each stage, by which the accuracy of the RS model is increased while reaching the global minimum. The response surface approximation is developed for the objective function. The optimization is carried out with the constraint given in equation (32). The dynamic stress constraints are evaluated at the optimal design point and the optimization process is terminated when one of the dynamic stress constraints become active. In the two design variables case, the dynamic stress constraints are not critical within the design space. Therefore, response surface approximations are not created for the dynamic stress constraints. However, if the design variables are more, then the dynamic stress constraint sensitivities may be moderate. Therefore, the response surface approximations have to be created for them and used as constraints in the optimization process. The stages of optimization for two design variables are discussed below.

In the first stage of optimization, a variation of 25 and 5 percent is taken from the baseline values of torsional stiffness and the mass of the blade, respectively. Then, the optimization if carried out as discussed in the quasi-steady state case. The RS model developed for this stage is shown in the Fig.3. The Hessian corresponding to this quadratic form is indefinite. Therefore, one cannot conclude that the problem is convex and the optimal point may lie on the constraint boundary.

Table-2 : Genetic Algorithm Parameters

Algorithm Parameter	Value
Population size	50
Mutation rate	0.03
Crossover rate	0.5
Penalty factor	100

In this stage, the J_v is reduced by 7.15 percent from its initial value, for the values of design variables, GJ = 0.007 and m = 1.065. The results obtained in this case show that value of mass has to be increased and torsion stiffness also increased slightly from the initial baseline design value for reduction in the objective function value. Also, the RS model developed for the above two cases (shown in Fig.2 and Fig.3) are different, with in the same design space. This is found to be because of the strong influence of torsional stiffness, on the unsteady impulsive pitching moments. This clearly shows the significance of the unsteady aerodynamic model in the optimization process. The adequacy of the model developed is checked. The residuals versus fitted values is plotted for the model developed, as given in Fig.4. The plot does not reveal any obvious pattern and therefore the response surface chosen is adequate.

The optimum values of the first stage are taken as the initial design values for the next stage. The perturbations in m and GJ are made progressively smaller as the iteration progress. At the second stage, the design space is created with a variation of 15 and 3 percent along the torsional stiffness and the mass, respectively. In each stage, the constraints (27) and (28) are checked and the optimization is proceeded. In the third stage, a variation of 5 and 1

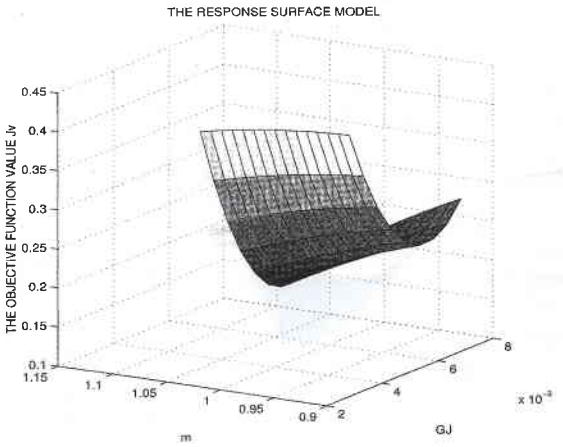

Fig.3 RS with unsteady model about baseline design ($\Delta GJ = 25\%$,$\Delta m = 5\%$) $J_v = 0.0232 - 177.95\, GJ + 2.208\, m + 24113.19\, GJ^2 - 0.88\, m^2 - 156.1\, GJ * m$

percent are taken in the torsional stiffness and mass respectively. The RS model developed for the second stage is shown in the Fig.5. Again, the RS is indefinite. The residuals versus the fitted values for the model in Fig.5 is shown in Fig.6. The RS model developed for the third stage is shown in the Fig.7. The residual versus the fitted values for the model in Fig.7 is shown in Fig.8. In both the Figs. 6 and 8 the plot does not reveal any obvious pattern. So the response surface models developed are considered to be adequate.

A reduction of 5.28 and 3.31 percent is achieved in the second and third stage, respectively. At the third stage, the constraint J_{dl} becomes active and the optimization process is terminated. Finally, a total reduction of 15.74 percent is achieved, for the objective function J_v. This is accomplished through three stages of optimization where response surfaces are created and GA is used for optimization. Since the RS models created are simple polynomials, GA finds the global constrained minimum point very rapidly. The interactive nature of the design process allows the termination of the optimization process at any stage with a feasible optimal design. The approach is therefore well suited for an industry setting.

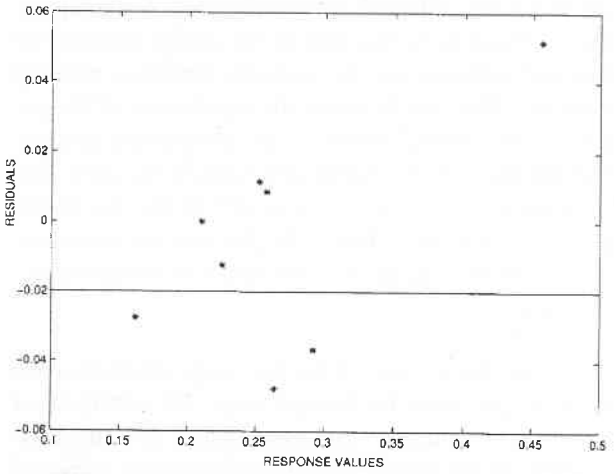

Fig.4 Plot of residuals versus fitted values for model, $J_v = 0.0232 - 177.95\ GJ + 2.208\ m + 24113.19\ GJ^2 - 0.88\ m^2 - 156.1\ GJ{*}\ m$

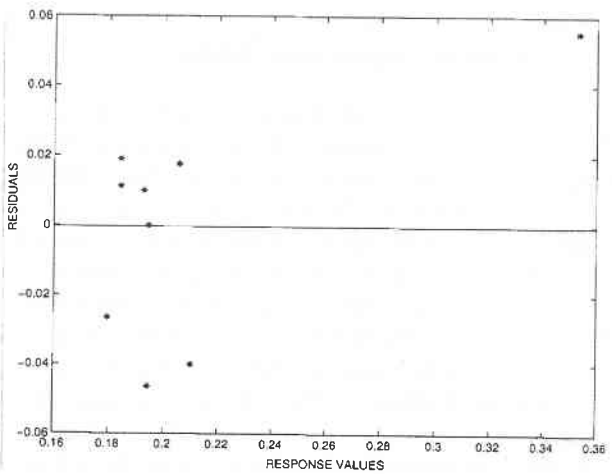

Fig.6 Plot of residuals versus fitted values for model, $J_v = 2.1877 + 1126.89\ GJ - 10.433\ m + 8939.8\ GJ^2 + 8.3184\ m^2 - 1159.37\ GJ{*}\ m$

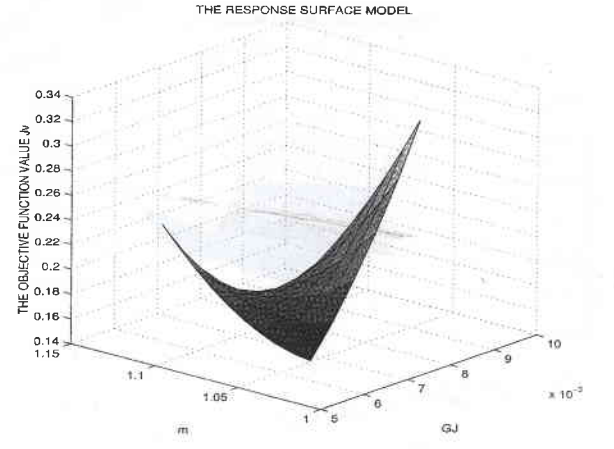

Fig.5 RS model for second stage $(\Delta\ GJ = 15\%\ ,\Delta\ m = 5\%)\ J_v = 2.1877 + 1126.89\ GJ - 10.433\ m + 8939.8\ GJ^2 + 8.3184\ m^2 - 1159.37\ GJ{*}\ m$

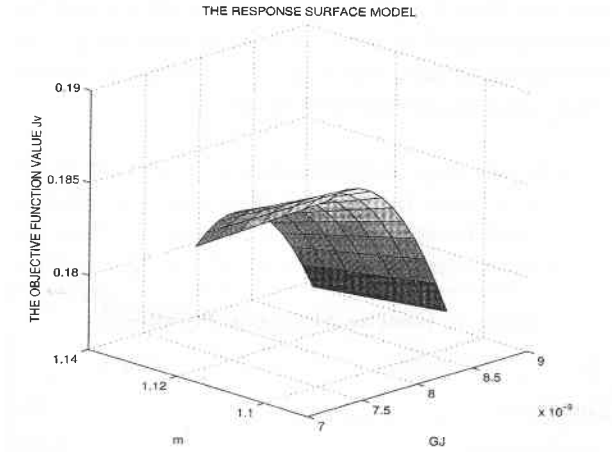

Fig.7 RS model for third stage $(\Delta\ GJ = 5\%\ ,\Delta\ m = 1\%)\ J_v = 0.7314 + 19.4041\ GJ - 0.9939\ m - 9632.49\ GJ^2 + 114.4797\ GJ{*}\ m$

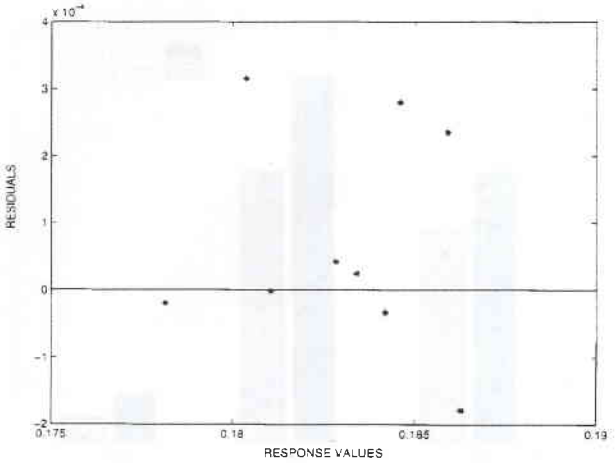

Fig.8 Plot of residuals versus fitted values for model, $J_v = 0.7314 + 19.4041\ GJ - 0.9939\ m - 9632.49\ GJ^2 + 114.4797\ GJ * m$

Four Design Variables

In this stage, two more design variables, the flap stiffness and the lag stiffness of the rotor blades are added in the optimization process. The flap stiffness and the lag stiffness of the blade are kept constant for the full span of the blade. Thus the four design variables are blade mass, flap, lag and torsional stiffness. A variation of 25 percent is taken for each of these stiffness variables and 5 percent along the mass design variable. For the four design variables, the axial distance in CCD is taken as $\sqrt{4}$. And the function is evaluated at 25 (2^4 + 2*4+1) design points. With these function values, RS model created is given below.

$$J_v = 64.7222 - 2756.55EI_y + 967.1EI_z - 2631.32GJ - 101.48m + 11769.52EI_y^2 + 1706.31EI_z^2 + 39111.5GJ^2 + 36.16m^2 - 14344.56EI_y * EI_z + 2562.96m*EI_y + 37308.78GJ * EI_y + 2333.35GJ * m - 730.43EI_z * m - 24278.09EI_z * GJ \quad (35)$$

Here also the RS turns out to be indefinite. The RS function with the constraints (4) and (5) is then minimized using the GA. A reduction of 14.85 percent in the optimum function value is achieved in the first stage with the dynamic constraint J_{d1} becomes active.

The results from the optimization, using four design variables are presented in Table-3. At the optimum, the frequencies are reduced as shown in the Table-4. The initial value of third flap frequency is close to 8/rev. The optimizer moves the design such that the third flap is away from the 8/rev. However, the second flap comes closer to 3/rev but the net result is such that vibration decreases. It has been observed in many earlier works that a decrease in torsional stiffness plays an much stronger role in vibration reduction than changes in flap stiffness. This is because the changes in blade elastic twist results in unloading of the blade at certain points in the azimuth. Further, the flap mode is highly damped due to aerodynamics compared to the low damped lag and torsion modes.

The vibration reduction is achieved by de-stiffening of the blade in flap, lag and torsion directions and a small increase in blade mass. The frequencies of the lag, flap and torsion mode are reduced from the baseline values. Fig.9 shows the 4/rev hub forces for the baseline and optimal design. Fig.10 shows the 4/rev hub moments for the baseline and optimal design. The dominant component of the 4/rev hub forces in this case is the 4/rev vertical shear and is reduced by 23 percent. This comes at the expense of a increase of 51.8 percent and 35 percent in the longitudinal and lateral 4/rev hub forces respectively. Fig.10 shows the 4/rev hub moments for the baseline and optimal design. The dominant component of the 4/rev hub moments are the rolling and pitching moments in this case. These are reduced by 22.5 and 26 percent, respectively. The relatively smaller yawing moment is also reduced by 49.7 percent. According to the Chattopadhyay et.al [11], among all the dynamic rotor hub loads, in general, the pitching and rolling moment contribute most significantly

Table-3 : Optimum Values (non-dimensionalised)

	Reference	At Optimum
EI_y	0.0108	0.0062
EI_z	0.0268	0.0134
GJ	0.00615	0.0033
m	1.0	1.0999

Table-4 : Blade Frequencies (per rev)

Mode	Reference	At Optimum
First Lag	0.744	0.579
First Flap	1.146	1.105
Second Flap	3.512	3.097
Third Flap	7.944	6.442
First Torsion	4.551	3.223

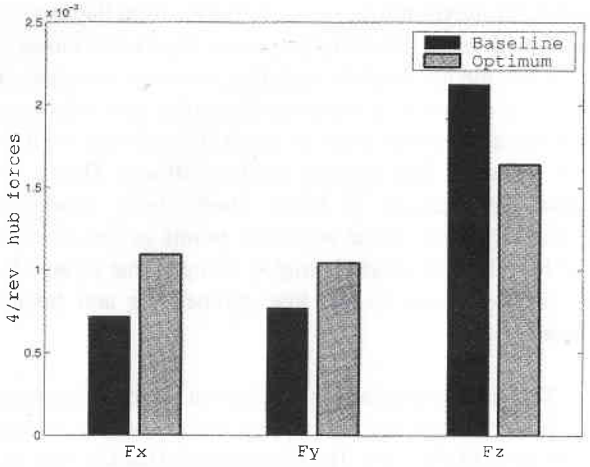

Fig.9 Vibratory forces on the rotor hub

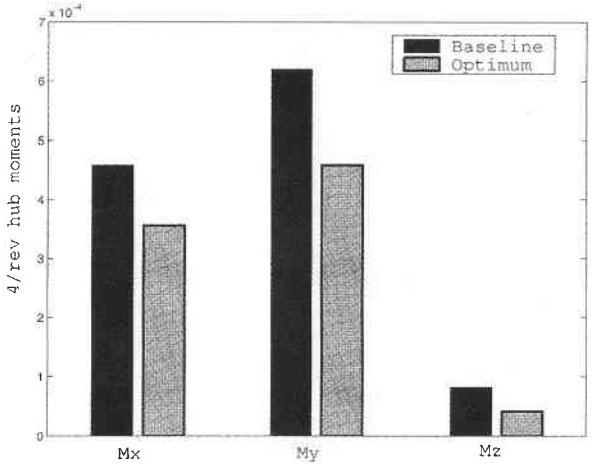

Fig.10 Vibratory moments on the rotor hub

to vehicle vibration. Also the vertical shear is a critical source of hub vibration. Therefore, the optimal design obtained is a good design.

Convergence problems were encountered in the aeroleastic analysis, at a few points identified by the CCD, when using the unsteady aerodynamics model. Therefore, the rotorcraft aeroelastic analysis was converged with a relaxed convergence criteria at these points. The fragility of rotor aeroleastic analysis, when sophisticated aerodynamic models are used has been noted by some researchers [48, 49]. This problem is very important for the successful application of optimization to rotor aeroelastic problems. If the rotor aeroelastic analysis fails to converge at any point, typical optimization algorithms based on gradient or non-gradient methods will have serious problems. The 'divergence' of a non-linear analysis results in the 'divergence' of the entire optimization process. However, when constructing response surface approximations, the rotor designer is able to use his or her experience in tuning convergence parameters or initial guesses for the analysis to obtain a reasonable load prediction. Therefore, the interactive development and use of response surface approximations for the rotor aeroelastic analysis allows the use of optimization methods in helicopter industry.

Conclusions

The problem of vibration reduction in a 4-bladed rotor is solved using a response surface approach. The objective function are the 4/rev hub loads. Constraints are imposed on blade root dynamic stresses and bounds are placed on the design variables to keep them in the region where the response surface approximation is valid. The following conclusions are drawn from this study.

1. Second order polynomial approximations based on the central composite design are effective for rotor aeroelastic analysis, provided the design variables are restricted to a region of validity.

2. The problems of numerical fragility of rotor aeroelastic analysis, especially when refined aeroelastic analysis are used, are easier to handle using the response surface approach which overfits a second order function and is therefore able to handle errors which may results in a few points due to lack of convergence.

3. The response surface approach decouples the analysis problem from the optimization problem and can help in spreading the use of optimization methods as a design tool in the helicopter industry, where one group can develop the approximations and another group can solve the optimization problems.

4. Using the blade flap, lag and torsion stiffness, and blade mass as design variables, it is found that vibration reduction of about 15 percent is obtained using just one response surface approximation. The final design is softer in flap, lag and torsion and showed a small increase in the mass. The dominant dynamic loads which are the vertical hub shear, and rolling and pitching moments show reduction of 23, 22.5 and 26 percent, respectively.

References

1. Ganguli, R. and Chopra, I., "Aeroelastic Optimization of Helicopter Rotor with Two Cell Composite Blades", AIAA Journal, 34 (4), 1996, pp.835-854.

2. Ganguli, R. and Chopra, I., "Aeroelastic Optimization of Helicopter Rotor with Composite Coupling", Journal of Aircraft, 32 (6), 1995, pp.1326, 1334.

3. Yuan, K-A. and Friedmann, P.P., "Structural Optimization for Vibratory Loads Reduction of Composite Helicopter Rotor Blades with Advanced Geometry Tips", Journal of the American Helicopter Society, 43 (3), 1998, pp.246-256.

4. Yuan, K-A. and Friedmann, P.P., "Aeroelasticity and Structural Optimization of Helicopter Rotor Blades with Swept Tips", NASA CR-4465, 1995.

5. Chattopadhyay, A. and Walsh, J.L., "Minimum Weight Design of Rotorcraft Blades with Multiple Frequency and Stress Constraints", AIAA Journal, 28 (3), 1990, pp.565-567.

6. Chattopadhyay, A., Walsh, J.L. and Riley, M.F., "Integrated Aerodynamic Load/Dynamic Optimization of Helicopter Rotor Blades", Journal of Aircraft, Special issue on Multidisciplinary Optimization of Aeronautical Systems, II, 1991, pp.58-65.

7. Chattopadhyay, A., "Vibration Reduction in an Articulated Rotor Blade using Structural Optimization", Engineering Optimization, 19, 1992, pp.37-50.

8. Chattopadhyay, A. and McCarthy, T.R., "A Multidisciplinary Optimization Approach for Vibration Reduction in Helicopter Rotor Blades", Computers and Mathematics with Applications, 25 (2), 1993, pp 59-72.

9. McCarthy, T.R., Chattopadhyay, A., Talbot, P. and Madden, J.F., "A Performance Based Optimization Procedure for High Speed Prop-rotors", Journal of the American Helicopter Society, 40 (3), 1995, pp.92-100.

10. McCarthy, T.R. and Chattopadhyay, A., "A Coupled Rotor/Wing Optimization Procedure for High Speed Tilt Rotor Aircraft", Journal of the American Helicopter Society, 41 (4), 1996, pp.360-369.

11. Chattopadhyay, A., "Vibration Reduction in Rotor Blades Using Active Composite Box Beam", AIAA Journal, 38 (7), 2000, 1125-1131.

12. Hajela, P., "Nongradient Methods in Multidisciplinary Design Optimization Status and Potential", Journal of Aircraft, 36 (1), 1999, pp.255-265.

13. Lee, J. and Hajela, P., "Parallel Genetic Algorithm Implementation in Multidisciplinary Rotor Blade Design", Journal of Aircraft, 33 (5), 1996, pp.962-969.

14. Kim, J.E. and Sarigul-Klijn, N., "An Application of Multidisciplinary Design Optimization to an Articulated Rotor Blade in High Speed", Proceedings of Opti-Conf 99, Newport Beach, 1999.

15. Kim, J.E. and Sarigul-Klijn, N., "Aeroelastic Optimization of an Articulated Rotor Blade", 36th Technical Meeting of SES, Dynamic Systems, 1999.

16. Kim, J.E. and Sarigul-Klijn, N., "Structural Optimization for Light-Weight Articulated Rotor Blade", Proceedings of the 41st AIAA/ASME/AHS SDM Conference, 2000.

17. Kim, J.E. and Sarigul-Klijn, N., "Elastic-Dynamic Rotor Blade Design with Multiobjective Optimization", AIAA Journal, 39 (9), 2001.

18. Soykasap, O. and Hodges, D.H., "Performance Enhancement of a Composite Tilt-Rotor using Aeroelastic Tailoring", Journal of Aircraft, 37 (5), 2000, pp.850-858.

19. Celi, R., "Optimization-Based Inverse Simulation of a Helicopter Slalom maneuver", Journal of Guidance, Control and Dynamics, 23 (2), 2000, pp.289-297.

20. Ribera, M. and Celi, R., "Maneuvering Free Wake Sensitivity for Design Optimization Applications", Proceedings of the 57th American Helicopter Society Annual Forum, Washington, DC, 2001.

21. Spence, A.M. and Celi, R., "Efficient Sensitivity Analysis for Rotary-Wing Aeromechanical Problems", AIAA Journal, 32 (12), pp.2337-2344, 1994.

22. Celi, R., "Recent Applications of Design Optimization to Rotorcraft - A Survey", Journal of Aircraft, 36 (1), pp.176-189, 1999.

23. Lu, Y. and Murthy, V.R., "Sensitivity Analysis of Discrete Periodic Systems with Applications to Helicopter Rotor Dynamics", AIAA Journal, 30 (8), pp.1962-1969, 1992.

24. Lim, J.W. and Chopra, I., "Aeroelastic Optimization of a Helicopter Rotor using an Efficient Sensitivity Analysis", Journal of Aircraft, 28 (1), pp.29-37, 1991.

25. Patrick, N.K., "Statistical Approximations for Multidisciplinary Design Optimization : The Problem of Size", Journal of Aircraft, 36 (1), pp.275-286, 1999.

26. Venter, G., Haftka, R.T. and Starnes, Jr. J.H., "Construction of Response Surface Approximations for Design Optimization", AIAA Journal, 36 (12), pp.2242-2249, 1998.

27. Hosder, S., Watson, L.T., Grossman, B., Mason, W.H., Kim, H., Haftka, R.T. and Con, S.E., "Polynomial Response Surface Approximations for the Multidisciplinary Design Optimization of a High Speed Civil Transport", Optimization and Engineering, 2 (4), pp.431-452, 2001.

28. Henderson, J.L., Walsh, J.L. and Young, K.C., "Applications of Response Surface Techniques to Helicopter Rotor Blade Optimization Procedure", Proceedings of the AHS National Technical Specialist Meeting on Rotorcraft Structures, Design Challenges and Innovative Solutions, Williamsburg, VA, 1995.

29. Ganguli, R. and Chopra, I., Aeroelastic Optimization of Helicopter Rotor to Reduce Vibration and Dynamic Stresses", Journal of Aircraft, 12 (4), pp.808-815, 1996.

30. Goldberg, D.E., "Genetic Algorithms in Search, Optimization and Machine Learning", Addison-Wesley, 1989.

31. Hodges, D.H. and Dowell, E.H., "Nonlinear Equations of Motion for the Elastic Bending and Torsion and Twisted Non-uniform Blades", NASA TND-7818, 1974.

32. Chopra, I. and Sivaneri, N.T., "Aeroelastic Stability of Rotor Blades using Finite Element Analysis", NASA CR 166389, 1982.

33. Hansford, R.E., "A Uniform Formulation of Rotor Loads Prediction Methods", Journal of the American Helicopter Society, Vol.31, pp.58-65, 1986.

34. Ganguli, R., Aeroelastic Optimization of Advanced Geometry and Composite Helicopter Rotors", Ph.D. Dissertation, University of Maryland at College Park, MD, USA, 1994.

35. Johnson, W., Helicopter Theory, Princeton University Press, Princeton, NJ, USA, 1980.

36. Borri, M., "Helicopter Rotor Dynamics by Finite Element Time Approximations", Computer and Mathematics with Applications, 12A (1), pp.149-160, 1986.

37. Bir, G. et.al., "University of Maryland Advanced Rotorcraft Code (UMARC) Theory Manual", UM-AERO Report 92-02, 1992.

38. Myers, R.H. and Montgomery, D.C., "Response Surface Methodology : Process and Product Optimization using Designed Experiments", Wiley, New York, 1995.

39. Crossley, W.A., Wells, V.L. and Laananen, D.H., "The Potential of Genetic Algorithms for Conceptual Design of Rotor Systems", Engineering Optimization, 24 (3), pp.221-238, 1995.

40. Crossley, W.A., Regulski, J.J., Wells, V.L. and Laananen, D.H., "Incorporating Genetic Algorithms and Sizing Codes for Conceptual Design of Rotorcraft", Proceedings of the American Helicopter Society Vertical Lift Aircraft Design Conference, San Francisco, CA, 1.4.1-1.4.14, 1995.

41. Crossley, W.A., "Genetic Algorithm Approaches for Multiobjective Design of Rotor Systems", Proceedings of the AIAA/NASA/ISSMO 6th Symposium on

Multidisciplinary Analysis and Optimization, Bellevue, WA, AIAA, Reston, VA, 384-394.

42. Crossley, W.A., "A Genetic Algorithm with the Kreisselmeier-Steinhauser Function for Multiobjective Constrained Optimization of Rotor Systems", Proceedings of the AIAA 35th Aerospace Sciences Meeting and Exhibit, Reno.NV, AIAA, Reston, VA, 1997.

43. Crossley, W.A. and Laananen, D.H., "The Genetic Algorithm as an Automated Methodology for Helicopter Conceptual Design", Journal of Engineering Design, 8 (3), pp.231-250, 1997.

44. Crossley, W.A. and Laananen, D.H., "Conceptual Design of Helicopters via Genetic Algorithm", Journal of Aircraft, 33 (6), pp.1062-1070, 1996.

45. Wells, V.L., Han, A.Y. and Crossley, W.A., "Acoustic Design of Rotor Blades Using a Genetic Algorithm", Aerodynamics and Aeroacoustics of Rotorcraft, AGARD, CP-552, pp.1-10, 1995.

46. Coello, C.A., "Theoretical and Numerical Constraint handling Techniques used with Evolutionary Algorithms : A Survey of the State of the Art", Computer Methods in Applied Mechanisms and Engineering, 191, pp.1245-1287, 2002.

47. Leishman, J.G. and Beddoes, T.S., "A Semi-Empirical Model for Dynamic Stall", Journal of the American Helicopter Society, 34 (3), pp.3-17, 1989.

48. Tarzanin, F. and Young, D.K., "Boeing Rotorcraft Experience with Rotor Design and Optimization", AIAA-98-4733.

49. Tarzanin, F., Young, D.K. and Panda, B., "Advanced Aeroelastic Optimization Applied to an Improved Performance, Low Vibration Rotor", Proceedings of the 55th American Helicopter Society Annual Forum, Montreal, Canada, 1999.